R. Hubo, A. Halim*, and W. Dahl**

Influence of Notch Acuity on the Temperature Dependence of Fracture Mechanics Values

REFERENCE Hubo, R., Halim, A., and Dahl, W., **Influence of notch acuity on the temperature dependence of fracture mechanics values**, *Defect Assessment in Components – Fundamentals and Applications*, ESIS/EGF9 (Edited by J. G. Blauel and K.-H. Schwalbe) 1991, Mechanical Engineering Publications, London, pp. 781–793.

ABSTRACT Fracture mechanics tests with different kinds of specimens have been performed to study the influence of specimen geometry and notch acuity on the fracture mechanics transition curve of three steels (Fe 510, FeE 690, FeE 885). Tests on specimens containing a blunt notch with a notch tip radius of 0.1 mm instead of a fatigue crack lead to an increase of the J_i values of 30–50 percent. The slope of the transition curve remains unchanged. The transition temperature T_i is shifted about 10 K to lower temperatures with decreasing notch acuity. The use of J_c and J_i values obtained from notched specimens for a failure prediction of wide plates containing notches with identical notch-tip radius as used in the small scale specimens leads to unsafe predictions. This result may be explained by differences of the local constraint although the notch acuity was equal. Finite element (FE) calculations with refined meshes for calculation of meaningful local stresses and strains will answer this question.

Introduction

A fracture mechanics based failure analysis (K, CTOD, or J analysis) requires the knowledge of material values describing the response of the material to the actual loading situation in the structure. The conservatism of the final statement about the safety of a structure strongly depends on the quality of the simulation of the constraint in the small scale specimen used for the evaluation of material values.

The influence of several geometry parameters like specimen thickness B, width W, overall dimensions, specimen type, side grooving and crack length a_0 on fracture mechanics material values and on crack resistance curves has been investigated by several authors **(1)–(5)**. In all cases fatigue cracks have been used to simulate a very severe loading situation. This seems to be quite reasonable due to the fact that fatigue cracks are often found in real structures. The assessment of components containing small notches instead of fatigue cracks often leads to very conservative estimations of tolerable defect sizes, loads, or minimum service temperatures, resulting from low material values due to a higher constraint in the prefatigued specimens compared to the notched component.

The investigations presented in this paper should show the influence of using notches instead of fatigue cracks, sidegrooving and specimen thickness on the J integral material values and the assessment of wide plate test results.

* Institute of Ferrous Metallurgy, Technical University Aachen, 5100 Aachen, FRG.

Material, specimen geometry, and testing procedure

Thirty mm thick plates of structural steels of grade Fe 510, FeE 690, and FeE 885 were used for this investigation. Table 1 shows the chemical composition of the steels. The microstructure of the Fe 510 steel mainly contains ferrite and pearlite with additional bainite-martensite areas spreaded inhomogeneously in the centre of the plate. The waterquenched and tempered high strength steels show a tempered bainite–martensite microstructure. The mechanical properties in transverse direction (mid-thickness) are given in Table 2. The yield strength varied between 401 MPa (Fe 510) and 923 MPa (FeE 885). The upper shelf value of the Charpy impact energy is 200 J for the Fe 510 steel and 73 J and 83 J, respectively, for the high strength steels.

Different kinds of fracture mechanics specimen were taken from the base plates to vary loading conditions (bending, combined bending, and tension), thickness (13 mm to 28 mm) and notch acuity. The 10 series of specimens shown in Table 3 have been prepared from the steel FeE 690.

Sidegrooved and prefatigued CT (compact tension) and SECB (single edge cracked bend, $W = 2B$) specimens **(6)(7)** of 25mm thickness were used for the series 1 and 2. The SECB specimens of series 3 had a thickness of 28 mm which is nearly the original plate thickness. For series 4, 5, and 6, 28 mm thick specimens with a notch instead of a fatigue crack have been prepared (notched CT = NCT, single edge notched bend = SENB). The notch tip radius of 0.1 mm was chosen according to the notch tip geometry used in wide plates which should be assessed on the basis of the small scale test results. The original plate thickness was reduced to 13 mm for series 7–10. The CT and SECB specimens of series 7 and 9 were taken from subsurface (ss) position whereas for series 8 and 10 the specimens were sampled from the mid-thickness position (mt). The a/W ratio of all specimens was very similar showing values

Table 1 Chemical composition (wt%)

Steel	*C*	*Si*	*Mn*	*P*	*S*	*Al*	*Cu*	*Cr*	*Ni*	*V*	*Mo*
Fe 510	0.2	0.47	1.56	0.021	0.002	0.033	0.07	0.05	0.03	—	—
FeE 690	0.18	0.61	0.95	0.013	0.004	0.066	—	0.91	—	—	0.42
FeE 855	0.16	0.27	0.76	0.007	0.001	0.025	—	0.60	1.87	0.06	0.41

Table 2 Mechanical properties at 293 K (transverse, mid-thickness)

Steel	σ_{YS} (*MPa*)	σ_{UTS} (*MPa*)	A_5 (%)	Z (%)	CVN_{max} (*J*)	$T_{50\%CVNmax}$ (*K*)
Fe 510	401	594	28	75	200	236
FeE 690	748	827	18	64	73	218
FeE 855	923	995	18	69	83	215

Table 3 Geometry and sampling position of specimens

Series No	*Type of specimen*	*Notch (N) Crack (C)*	*Thickness mm*	*Side grooves (%)*	*Sampling position*
1	1 CT	C	25	20	approximately full thickness
2	SECB	C	25	20	approximately full thickness
3	SECB	C	28	—	full thickness
4	1 NCT	N	28	—	full thickness
5	SENB	N	28	—	full thickness
6	SENB	N	28	20	full thickness
7	1 CT	C	13	20	subsurface
8	1 CT	C	13	20	mid-thickness
9	SECB	C	13	20	subsurface
10	SECB	C	13	20	mid-thickness

Series 1 and 4 have also been tested for the steels Fe 510 and FeE 885.

between 0.53 and 0.55. The orientation was T–L compared to the rolling direction. The quasistatic tests were performed at different temperatures to get a complete fracture mechanics transition curve. J_c values have been determined below the transition temperature T_i, at which the first amount of stable crack extension can be observed on the fracture surface. J_i values have been evaluated with the direct current potential drop technique (DCPD) at temperatures beyond T_i. Cleavage fracture after a small amount of stable crack extension gave J_u values and in the upper shelf area J_{max} values were determined if the plastic collapse load had been reached.

Fracture mechanics transition curves

The first part of this paragraph is concerned with the results of test series 1–10 on the steel FeE 690. At the end the results of tests on the two other steels are presented.

Figure 1 shows a comparison of the J integral transition curves of steel FeE 690 which have been determined with test series 1 and 2. The only difference between both series is the type of loading which is combined tension and bending for the CT specimens (series 1) and three-point bending for the SECB specimens (series 2). The results of both series can be described by one common scatterband. The scatter in the transition area is quite large, with differences of the J values at the same temperature up to 100 percent. Separations have been observed in the centre of the specimens at temperatures above 223 K (see Fig. 2). The formation of separations is supported by the sidegrooves leading to high stresses in z direction. The separations caused only small pop-ins with a drop of the load smaller than 5 percent. The occurrence of separations is one reason for the relatively large scatter of tests results in the transition area. The specimens with a centre line separation showed higher J_c and J_u values resulting from effectively testing two separate thin specimens

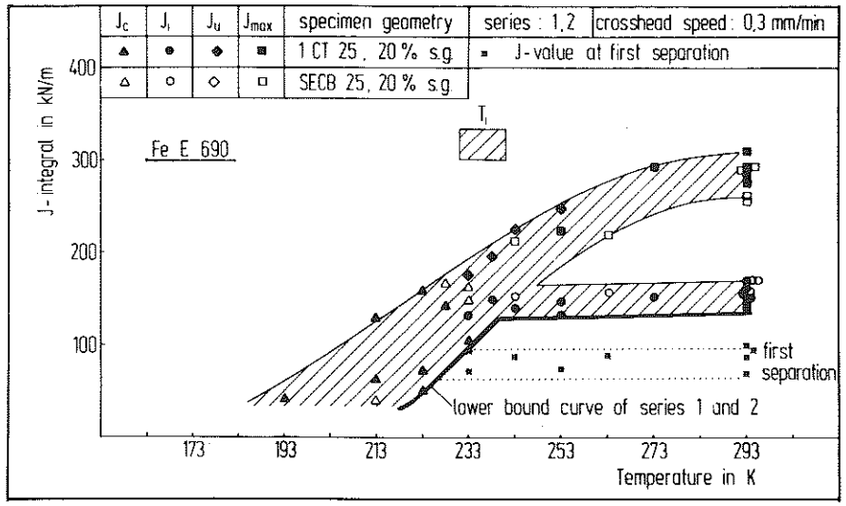

Fig 1 ***J*** **integral as a function of temperature of test series 1 and 2 (FeE 690)**

with a lower local constraint compared to the original specimen. The $J_{sep.}$ (sep. = separate) values, determined at the first occurrence of the centre line separation, lay between 65 kN/m and 95 kN/m. Even at the highest temperature of 293 K separations were observed. A slight increase of the $J_{sep.}$ values was found with increasing temperature. A similar result was observed for the J_i values. Values between 130 kJ/m and 160 kJ/m have been evaluated for the initiation of stable crack extension. The first amounts of ductile tearing appeared between 231 K and 241 K (T_i area). The J_{max} values (260–310 kN/m) showed no difference between CT and SECB specimens. This result is in contrast to results of former investigations **(8)**, where large differences between J_{max} values of CT and SECB specimens have been presented. The small differ-

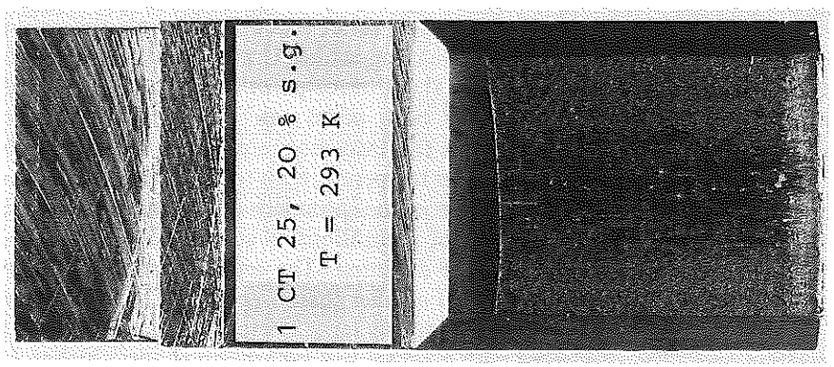

Fig 2 Fracture surface of a specimen tested at 293 K (separations, stable crack growth)

ences of the J_{max} values indicate very similar J_R curves of both types of specimens. This can be explained by the occurrence of separations dominating the fracture process in the centre of the specimen.

Figure 2 shows the fracture surface of a broken specimen tested at 293 K. Pronounced splittings in the centre of the specimen resulting in large amounts of stable crack extension underline the influence of the separations on the crack extension process. The assessment of the wide plate test results will be performed based on the lower bound curve of the J_c and J_i values (see Fig. 1).

Figure 3 shows a comparison of the scatterband of series 1 and 2 with the results of test series 3. The influence of an increased thickness (25 mm/sidegrooved – 28 mm/non-sidegrooved) can be neglected. Only the geometry-dependent J_u values of series 3 are higher than those of series 1 and 2 giving a steeper upper part of the transition curve. J_c, J_i, and J_{max} values of series 3 are included in the scatterband of series 1 and 2. The lower bound curves and T_i of all three series are identical.

The $J_{sep.}$ values are slightly higher for series 3 due to a lower local loading in z direction in the non-sidegrooved specimen **(9)**.

Test results of the notched CT (NCT) and the SENB specimens (series 4 and 5) are shown in Fig. 4. The differences between J_c and J_i values are negligible, as they were for the prefatigued specimens of series 1, 2, and 3. The lower bound curve of series 4 and 5 is shifted to higher J values (factor 1.5) and lower temperatures compared to the lower bound curve of series 1–3 The temperature shift of T_i is about 10 K. Beyond T_i the J_u values of the SENB specimens are slightly higher than those of the NCT specimens. The $J_{sep.}$ values are also increased by a factor of about 1.5 like the J_c and J_i values. This is an

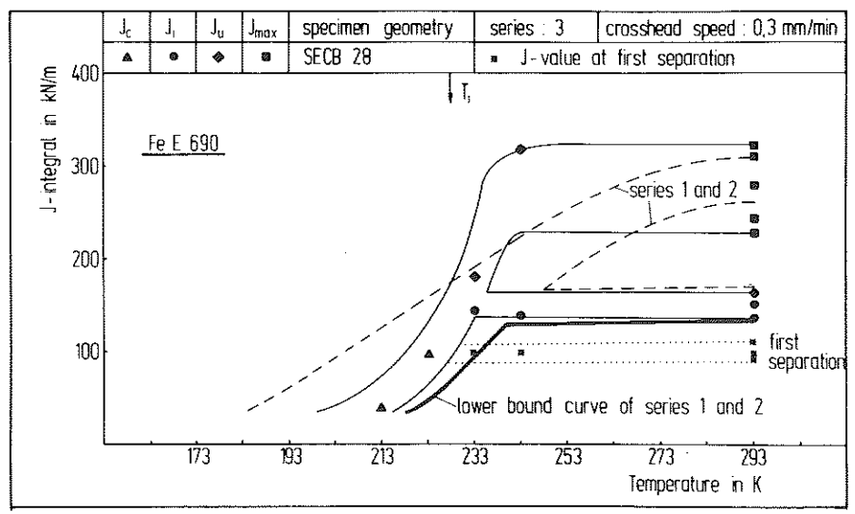

Fig 3 ***J*** **integral as a function of temperature of test series 3 (FeE 690)**

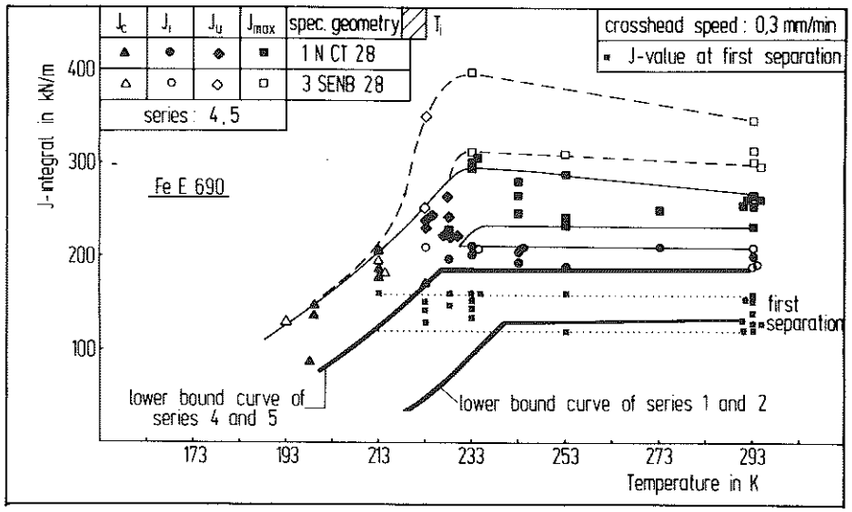

Fig 4 *J* integral as a function of temperature of test series 4 and 5 (FeE 690)

indication for the lower local constraint situation in front of the notch tip. The specimens of test series 6 (SENB 28) were 20 percent sidegrooved. A comparison of the results of test series 5 and 6 (see Fig. 5) showed no influence of the additional sidegrooving. All values belong to the scatterband of series 4 and 5.

At 293 K the J_{max} values and the amount of stable crack extension Δa at maximum load are very similar for all notched and prefatigued specimens of

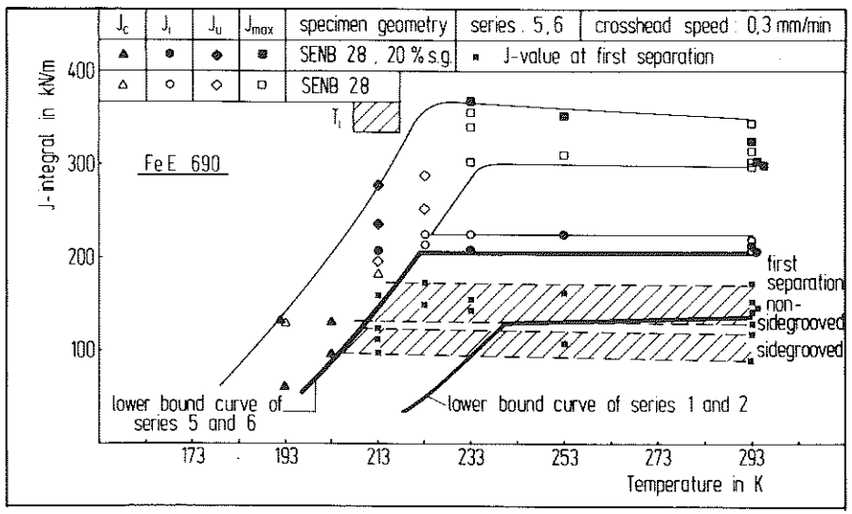

Fig 5 *J* integral as a function of temperature of test series 5 and 6 (FeE 690)

series 1–6. This indicates that the J–Δa curves for both notch acuities are nearly equal at this loading point. Further investigations have to clarify this result.

The background for the test series 7–10 was to show the influence of microstructure variations in the thickness direction. Therefore specimens were taken from sub-surface (ss) and mid-thickness (mt) position. A second reason for testing thin specimens was to clarify if a reduction of thickness only would give the same results as a proportional reduction of the specimen size. The CT specimens therefore got the dimensions of a standard 1 CT specimen except for the thickness of 13 mm. The SECB specimens were proportionally reduced to a thickness of 13 mm and a width of 26 mm ($W = 2B$). All specimens have been prefatigued and 20 percent sidegrooved.

A comparison of test results of series 7, 8 and 9, 10 are shown in Figs 6 and 7. For both types of specimens large differences between the transition curves for ss and mt positions have been evaluated. The transition temperature T_i of the ss position is about 30 K higher than that of the mt position, although the J values itself are higher for the ss position. One reason for the large differences may be the occurrence of phosphorus segregations discontinuously spread in mid-thickness areas of the plate. The comparison of CT and SECB specimens from the same sampling position shows that higher J values have been determined for the CT specimens resulting from the higher load bearing capacity of the CT specimens having a ligament length of twice the length of the SECB specimens.

The lower bound curves of series 1–3 and series 8 and 10, all evaluated by fatigue cracked specimens, showed no agreement of J_i values and T_i (see Fig.

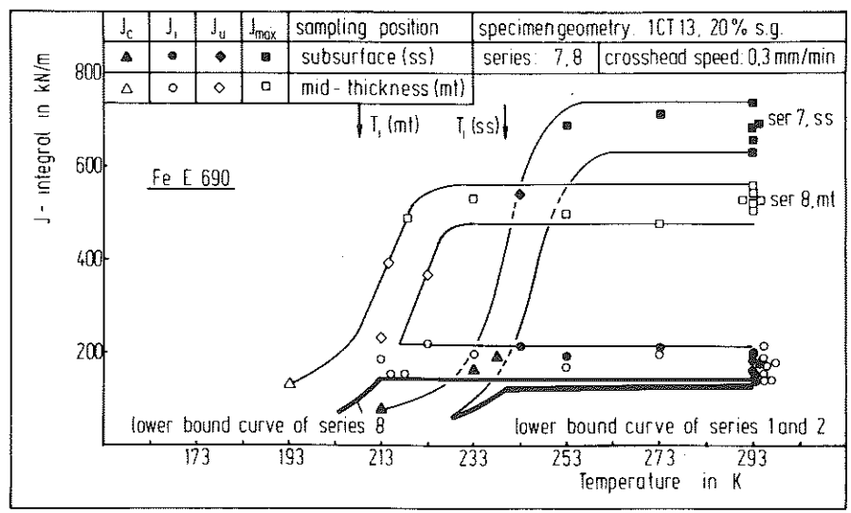

Fig 6 *J* integral as a function of temperature of test series 7 and 8 (FeE 690)

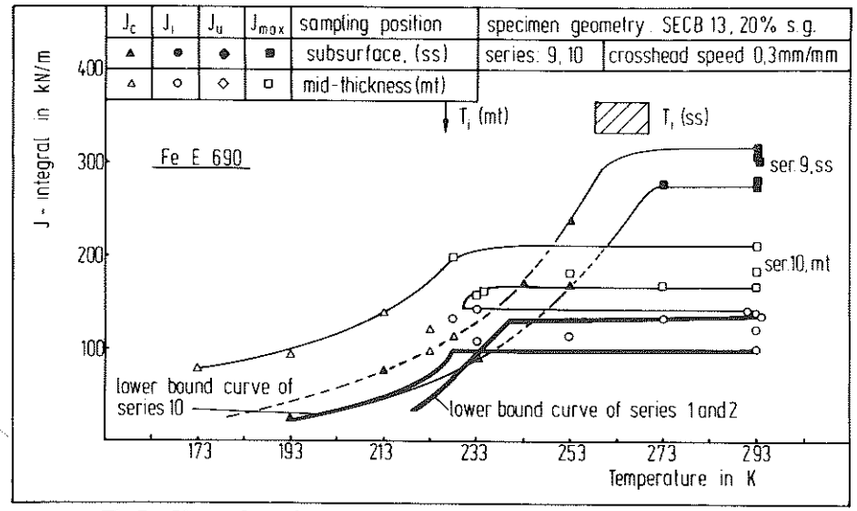

Fig 7 *J* integral as a function of temperature of test series 9 and 10 (FeE 690)

8). The J_i values of the series 8 (SECB 13) is lower than that of the full thickness specimens. The higher value of the full thickness specimens could be explained by supporting effects of the surface regions, which showed much higher J_i values. The lower bound curve of the 1CT13(mt) specimens shows in general higher J_c and J_i values due to the different local constraint (see previous paragraph). Also for the transition temperature T_i differences up to 15 K have been found. It can be concluded from this result that the use of J values

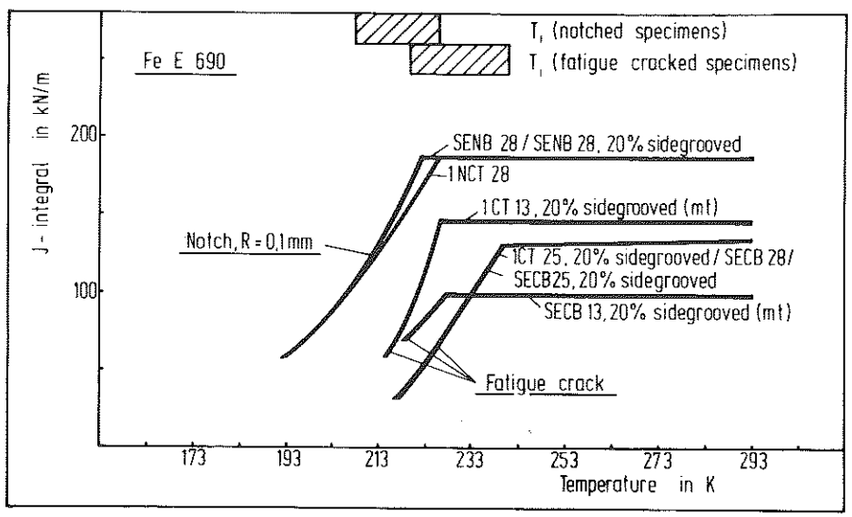

Fig 8 Comparison of lower bound curves of different test series of the steel FeE 690

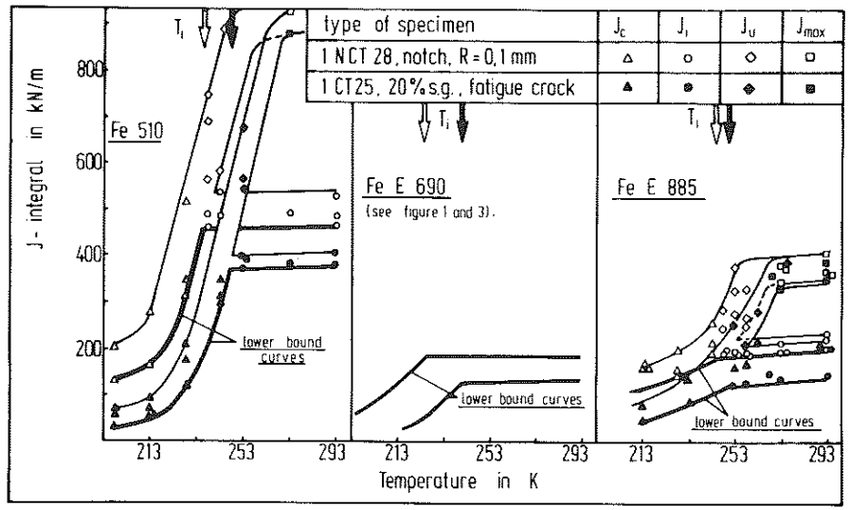

Fig 9 *J* integral as a function of temperature of test series 1 and 4 of the steels Fe 510, FeE 690, and FeE 885

and T_i of thin specimens for the assessment of components should be done carefully if variations of the material properties in the thickness direction can occur.

The influence of the notch tip acuity on the initiation values J_c and J_i which has been demonstrated in Fig. 4 for steel FeE 690 is confirmed by results of tests on the steels Fe 510 and FeE 885 (see Fig. 9). The large scatter of J values in the transition area of steel Fe 510 results from the discontinuously spread bainite–martensite islands in the centre of the plate of this steel **(10)**. The scatter of the steel FeE 885 in the transition area is relatively small. The difference of the transition temperature T_i of notched and cracked specimens is about 10 K. The J_i values of the notched specimens are increased by 30 percent to 50 percent. The factor of increase in the lower transition curve (J_c values) depends on the steepness of the curve. For a very steep transition curve the factor can be much higher than 1.5 whereas in a flat transition curve the factor of the J_i values remains the same for the increase of the J_c values. In general the results show, that the slope of the transition curves remains the same and a temperature shift of about 10 K for T_i has to be taken into account, if a notch with a tip radius of 0.1 mm is used instead of a fatigue crack.

Comparison of failure predictions and wide plate test results

In order to avoid problems arising from approximation methods for the determination of the crack driving force finite element calculations have been performed to evaluate $J_{appl.}$ values as a function of the applied load **(11)–(13)**. The

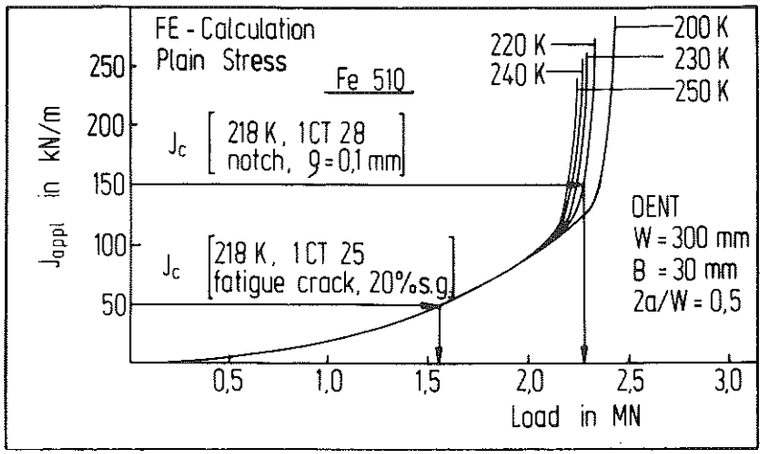

(a)

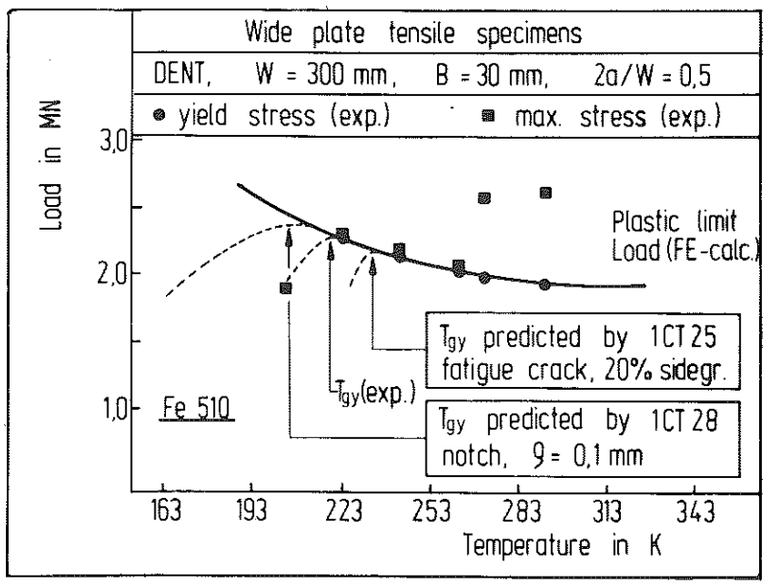

(b)

Fig 10 (a) Prediction of failure loads and transition temperature T_{gy} using FE calculations and test results of series 1 and 4 (b) Comparison of predictions and wide plate test results

elastic–plastic displacement controlled computations were carried out with the general purpose finite element program ABAQUS **(14)** utilising the von Mises yield condition and isotropic work hardening. The strength behaviour was represented by a multilinear approximation of the true stress–strain curve, in which the experimentally observed Lueders strain region was taken into account. Young's modulus amd Poisson's ratio were taken to be $E = 210$ GPa and $\nu = 0.3$, respectively. The J integral was calculated according to the virtual crack extension technique **(15)**. It has been demonstrated **(16)** that a plane stress solution is sufficiently precise if a failure analysis based on the J integral concept has to be performed for a wide plate of 30 mm thickness. The calculated geometry was of the DENT type (double edge notched tension) with a width $W = 300$ mm, a notch tip radius of 0.1 mm, and a total notch length $2a = 150$ mm. This geometry is identical with the geometry of the tested wide plates of steel Fe 510. The consequences for a failure assessment are demonstrated in Fig. 10, if lower bound fracture mechanics values of series 1 (1CT25, fatigue crack, 20 percent sidegrooved) and series 4 (1NCT28) are used. The upper part of Fig. 10 shows the calculated $J_{appl.}$ curves for different temperatures and as an example the determination of failure loads at 218 K using the above mentioned J_c material values. The lower part of Fig. 10 presents the experimentally evaluated general yield (net section yielding) and maximum loads and the predictions of failure loads.

A conservative prediction of failure loads and the transition temperature T_{gy} is made using the data of lower bound transition curve of the sidegrooved 1CT25 specimens (series 1). The use of the data of the notched specimens (lower bound transition curve of series 4) leads to a shift of T_{gy} to lower temperatures. In this case an underestimation of T_{gy} is observed, but it has to be taken into account, that the accuracy of the experimental determination of T_{gy} strongly depends on the temperature interval between two tests, which in this case was 20 K. Without carrying out the procedure for assessing the failure behaviour the shift of the predicted T_{gy} can already be gathered from the upper part of Fig. 10, beacuse in one case (data of series 4) general yield is reached at 218 K and in the other case (data of series 1) the critical J value still belongs to the small scale yielding region of the wide plates. Thus brittle failure is predicted at 218 K.

Summary and conclusions

Fracture mechanics tests with different kinds of specimens have been performed to study the influence of the type of the specimen (CT/SECB), the thickness (13/25/28 mm), sidegrooving, the sampling position (full thickness/subsurface/mid-thickness) and in particular the influence of the notch acuity (fatigue crack/notch, $R = 0.1$ mm) on the fracture mechanics transition curve of a structural steel FeE 690. In addition the influence of the notch acuity has also been investigated on steels of grade Fe 510 and FeE 885.

Large scatter in the transition range could be explained by microstructure variations in the thickness direction. A difference of the results from tests with CT and SECB specimens of the same thickness has not been found. The influence of the sampling position was large. No agreement between lower bound curves of full thickness tests and tests with specimens sampling the mid-thickness or the subsurface position has been obtained.

A transfer of J values or transition temperature T_i from thin to thick specimens therefore should be done very carefully if gradients of the material properties are existing in the thickness direction.

The tests on specimens containing a notch with a notch tip radius of 0.1 mm lead to higher J_c and J_i values compared to those of the prefatigued specimens. For all three steels the J_i value was increased by 30–50 percent. The slope of the transition curve remains unchanged. The transition temperature T_i is shifted about 10 K to lower temperatures with decreasing notch acuity.

The use of J_c or J_i values obtained by testing prefatigued specimens in failure assessment of notched wide plates leads to a more or less conservative prediction of the failure loads and the transition temperature T_{gy}. Unsafe predictions were made in case J_c or J_i values of notched specimens were used although the notch tip radius was identical to that of the notches in the wide plates. The main conclusion from this result is that it is not enough to simulate only the same notch tip acuity in the small scale specimen. In order to get a better understanding of the fracture process, FE computations have to be performed for specimens and components using substantially refined meshes and thus giving the possibility to calculate meaningful local stress and strain distributions. The local constraint could then be characterised more precisely to guarantee a most accurate transferability of the results from small scale tests to real structures.

References

(1) SUN, D. Z., DORMAGEN, D., and DAHL, W. (1985) Influence of specimen geometry on fracture mechanics values at the onset of stable crack extension, *Steel. Res.*, **56**(8), 445–449.

(2) WELLMANN, G. W. *et al.* (1988) Specimen thickness effects for elastic–plastic CTOD toughness of an A 36 steel, *ASTM STP 945* (Edited by D. T. Read and R. P. Reed) ASTM, Philadelphia, pp. 553–554.

(3) FAUCHER, B. and TYSON, W. R. (1988) A study of variability, size and temperature effects on the fracture toughness of an arctic-grade steel plate, *ASTM STP 945* (Edited by D. T. Read and R. P. Reed) ASTM, Philadelphia, pp. 164–178.

(4) SUN, D. Z. (1987) *Influence of state of stress and microstructure on elastic–plastic fracture mechanics values*, PhD Thesis, Technical University, Aachen.

(5) HALIM, A. (1989) *Influence of microstructure and state of stress on the fracture mechanisms of technical steels*, PhD Thesis, Technical University, Aachen.

(6) Standard test method for J_{Ic}, a measure of fracture toughness (1987) *ASTM E 813-87*, ASTM, Philadelphia.

(7) BS 5762 (1979) *Method for crack opening displacement testing*, British Standard Institution, London.

(8) HEUSER, A. and DAHL, W. (1984) Influence of specimen geometry on the results of fracture mechanics tests, *Materialprüfung*, **26**, 389–393.

(9) AURICH, D. and SOMMER, E. (1988) The effect of constraint on elastic–plastic fracture, *Steel Res.*, **59**(8), 358–367.

(10) DAHL, W. and EHRHARDT, H. (1988) Influence of state of stress on the deformation and fracture behaviour of structural steels in wide plate tests, *Stahl und Eisen*, **108**, 101–104.

(11) TWICKLER, R., TWICKLER, M., and DAHL, W. (1985) Numerical analysis of wide plate tests and its application for failure predictions using FEM, Proc. ECF 6, Amsterdam, pp. 715–727.

(12) HUBO, R., TWICKLER, R., and DAHL, W. (1989) Influence of state of stress on fracture mechanics properties and consequence for failure predictions, Proc. of ICF 7, Houston, Vol. 4, pp. 2509–2517.

(13) TWICKER, R. (1988) *Application of the Finite Element Method to the fracture analysis in material technology*, PhD Thesis, Technical University, Aachen.

(14) HIBITT, H. D., KARLSON, B. I., and SORENSEN, P. (1988) *ABAQUS Users Manual, Theory Manual, Version 4.7*, Providence RI, USA, HKS Inc.

(15) PARKS, D. M. (1977) The virtual crack extension method for non-linear material behaviour, *Comp. Meths Appl. Mech. Engng*, **12**, 353–364.

(16) DAHL, W. *et al.* (1985) Application of fracture mechanics concepts to the failure of wide plates, *Nucl. Engng Des.*, **87**, 83–88.